Investigation of Blue Shift Phenomena and Dielectric Behaviour With the Concentration of Co Doped in Zns Nanoparticles

Anupam Pramanick[1,a], Tapas Pal Majumder[1,b], Debabrata Bhadra[2,c]

[1] *Department of Physics, University of Kalyani, Kalyani-741245 (West Bengal), India*
[2] *Department of Physics, Bhairab Ganguly College, Kolkata-700056 (West Bengal), India*

[a] pramanickanupam@gmail.com
[b] tpmajumder1966@gmail.com
[c] bhadra.debabrata@gmail.com

Abstract

In this work undoped Zinc Sulphide (ZnS) nanoparticles (NPs) and doped with Cobalt (Co) having dopant concentration 0.5%, 1.0%, 1.5% have been synthesized by hydrothermal method, in which ethylenediamine (EDA) has used as capping agent. An investigation has been made on the changes of structural, optical, molecular as well as electrical properties, occurs due to doping. X-ray diffraction (XRD) patterns reveal the idea about formation of samples with crystalline nature having intense peaks which are consistent with the primary cubic phase of zinc blend and nano-sized particles. None of any peak corresponding to doped material Co was noticed which means the Co ions had been incorporated successfully without vast modulating the original crystal structure. In association with hexagonal phase was found due to weak signature of ZnS. It has been pointed out from UV-Visible spectra the value of optical gap energy is a function of Cobalt concentration and quantum confinement process occurred. The occurrence of blue shift phenomena has been confirmed by the observed variation of the optical gap range between 4.01 to 4.79 eV. FTIR spectra showed ZnS characteristics frequency band position did not exhibit any distinguished change with doping what acknowledged the Co was well substitution of Zn into ZnS NPs. In photo luminance (PL) spectra the PL intensity did respond appreciable with modifying the Co concentration. The agglomerated NPs with almost spherical shaped and elemental compositions with stoitiometric ratios were confirmed by Scanning Electron Microscope (SEM) images and Energy Dispersive X-Ray (EDX) spectra respectively. Measured values of AC conductivity increases with Co concentration at higher frequency range which may make these materials useful at high frequency regime. Therefore, conclusion can be done, these studied ZnS doped with Co materials can show their applicability in spinotronics and photo luminescent devices.

Keywords: Cobalt-doped ZnS, Photo luminance, Band-gap, Fourier Transform Infrared (FTIR), AC conductivity.
Received 27 January 2025; First Review 14 February 2025; Accepted 15 February 2025

*** Address of correspondence**
Anupam Pramanick
Department of Physics, University of Kalyani, Kalyani-741245 (West Bengal), India

Email: pramanickanupam@gmail.com

How to cite this article
Anupam Pramanick, Tapas Pal Majumder, Debabrata Bhadra, Investigation of blue shift phenomena and dielectric behaviour with the concentration of Co doped in ZnS nanoparticles, J. Cond. Matt. 2024; 02 (02): 46-52.

Available from:
https://doi.org/10.61343/jcm.v2i02.66

Introduction

In the last few decades most intensive research both theoretical and experimental is going on nanomaterials semiconductors in order to understand their marvelous optical, electrical and optoelectronics properties. ZnS is very popular semiconductor material due to its versatile characteristic's nature having two main crystalline forms, one is cubic (zinc blend) another is hexagonal. Among them cubic is more stable having band gap energy about 3.54 eV and 40 meV is the excitation binding energy whereas hexagonal has wider band gap of 3.91 eV. This duality helps ZnS for being outstanding polymer [1]. Apart from these, recent research on this material provides the information that it exhibits rhombohedral structure also [2]. For its luminescent property in photo electronic device, ZnS become very useful in the window materials [3], solar cell [4-5], laser diode [6-9].

The electrical, optical and magnetic properties of ZnS can be tuned with the suitable incorporation of rare earth (RM) and transition (TM) metals [10]. Last decades, efforts to have prepared ZnS NPs doped with TM and RM was very admirable [11-18]. The variation of the optical band gap energy E_g gambles on dopants type. TM metals have smaller ionic radii compared to Zn^{2+} and sp-d spin exchange interaction for which TM doped (Fe, Ni, Co, Cr) ZnS NPs have increased E_g [19-23] but doped with RM (Tb, Dy, Sm) dopants ZnS NPs got decreased E_g due to higher ionic radii and sp-f spin exchange [24-25].The d-orbital of Co mixes with the valence band and conduction band of the II-VI

materials that is why stronger coupling occurs in between Co and II-VI materials [26]. Apart these reports gathered from many researches the radii of Co^{2+} and Zn^{2+} are respectively 0.58 Å and 0.60 Å, as a result Co^{2+} substitutes Zn^{2+} at lattice site up to 15 at % to 20 at % in ZnS NPs without any drastic change of host lattice structure. So cobalt doped ZnS NPs are required investigation for structural, electrical, optical and magnetic properties [27]. Also, ZnS with Co NPs show paramagnetic and ferromagnetic nature depending on amounting of doping [28]. The hydrothermal method was chosen to employ here among the all-diverse types of synthesis process and several advantages [29-30].

In this work pure ZnS and doped with Co NPs have been prepared with different concentration of cobalt (0.5%, 1.0%, 1.5%). The main focus is to do analysis of the structural, electrical, molecular and optical, properties by using respectively XRD, UV-Visible, PL, FTIR, and dielectric measurement systems. SEM and EDX identified the morphologies and chemical composition.

Experimental Details

Sample Preparation

To synthesis required chemicals zinc acetate [$Zn(CH_3COO)_2.2H_2O$], thiourea [$(NH_2)_2CS$], cobalt chloride [$CoCl_2.6H_2O$] and EDA [$C_2H_8N_2$] which were analytical grade need not further purification. All glass wares were cleaned properly by using acid. Appropriate amount of Zn $(CH_3COO)_2.2H_2O$, $CoCl_2.6H_2O$ and $(NH_2)_2CS$, were deliquesced in eighty milliliter deionized water and EDA with same ratio of volume. For obtaining homogeneous by using magnetic stirrer mixture was agitated for 1 hour at normal temperature. After this solution was transformed to 100 ml silver lined stainless steel autoclave, filled 80% volume of it. Then the solution containing autoclave had been keeping furnace at temperature 200 °C for half of a day. After which it was conceded to settle naturally at acceptable temperature. Lastly obtained feculence consecutively filtered & then scrubbed by using ethanol and demineralized water several times. The final product was dried in oven at 100 °C for overnight. To have the (0, 0.5, 1.0 and 1.5) % Co concentrated ZnS NPs this synthesized process was conducted repeatedly.

Sample Characterizations, Outcome and Investigation:

Structural analysis

The nature of crystal structure, size of particle and phase have been investigated from the study of XRD pattern shown in Figure 1. The well-defined peaks at wide range of 2θ confirms self-prepared specimens are polycrystalline nature. From figure 1 the observed peaks of diffraction are located at about 27.16°, 28.87°, 30.48°, 39.67°, 47.56°, 52.03°, 56.60° which correspond to respectively (101), (008), (104), (108), (110), (1012) and (203) lattice planes of zinc blend and hexagonal wurtize structure and these are fit into with the standard JCPDS spectrum Card no. 72-0163. No Bragg's diffraction peak has detected for Co and its oxide, sulphide and any impurity indicating absence of any secondary phase, only single phase is dominant here and Co^{2+} ions doped successfully without considerable transforming the crystal structure of host materials ZnS. It has also noticed the peak intensity reduced gradually and broadening occurs which signifies the diminishes of crystalline quality of NPs due to distortion and induced strain because of doping of Co^{2+} ions into ZnS [31].

In conjunction with the diffraction peaks slightly shift towards higher 2θ values with compared to undoped ZnS nanocrystals. This might be due to substitution of Zn^{2+} ions by Co^{2+} in ZnS for which lattice constant could be reduced.

The reduction of lattice constant can be explained by the fact that Zn^{2+} has greater radius (0.074 nm) than that of Co^{2+} ions (0.072 nm). The average crystalline size was determined by Debye Sherrer's formula [32].

$$D = \frac{k\,\lambda}{ß\cos\theta} \qquad (1)$$

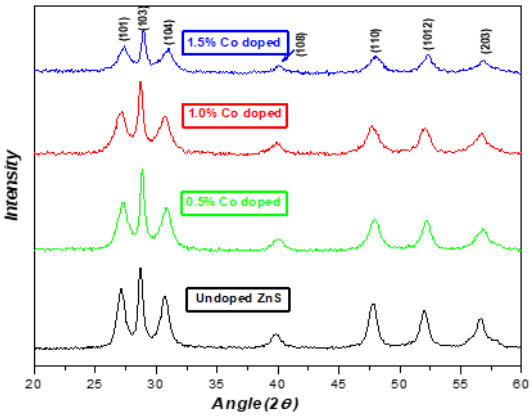

Figure 1: XRD of pure and Co concentrated ZnS NPs.

Where 'D' is dimension of the particle, 'k' serves as dimensionless constant with value 0.89, known as Sherrer's constant, λ (15.418 nm) is the wavelength of Cu-K_α, ß and θ are respectively line broadening corrected & Bragg's angle. The calculated crystalline size was gathered in Table 1 and the average crystalline dimension of pure and 0.5%, 1.0%, and 1.5% of Co doped ZnS were found to be 15.67 nm, 13.53 nm, 12.26 nm and 12.93 nm respectively. Thus, it is clear the average crystalline size reduces with greater concentration of Cobalt in the host materials.

Table 1: Data regarding structure of undoped and Co doped ZnS NPs from X-Ray Diffraction.

Co amount	2θ (degree)	crystalline size (nm)
Undoped	28.60	15.67
0.5%	28.84	13.53
1.0%	28.73	12.26
1.5%	28.92	12.93

Ultra Violet visible spectra and Optical Band Gap calculation

Figure 2 depicts the absorption spectra at room temperature for the samples of pure and Co concentrated ZnS was obtained in between wave length range from 200-800 nm. The blue shift in the absorption is attributed to the quantum size effect.

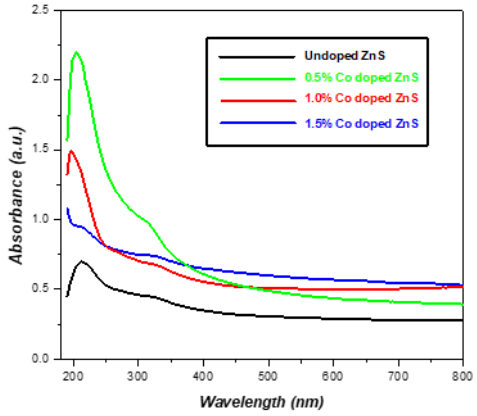

Figure 2: spectra of UV visible for Undoped and Co contained ZnS NPs.

Optical gap of pure and Co concentrated ZnS was made an estimate by using Tauc relation which is given by

$$\alpha h\nu = A(h\nu - E_g)^n \qquad (2)$$

Where α stands for co-efficient of absorption, Plank's constant is h, frequency of incident photon is ν, A taken as any constant whose value depends on characteristic transition and E_g is direct allowed band gap energy. The value of n depends on the nature of transition here with fitting value for ZnS is equal to $\frac{1}{2}$ which certifies conceded direct transition [33]. The curve of $(\alpha h\nu)^2$ vs hν has shown in the Figure, obtained energy gap values are 3.57, 4.45, 4.77 and 4.63 electron Volt respectively for pure and Co doped ZnS NPs which are more than that of band gap value of bulk ZnS (3.54 eV) [34] and this confirms the formation of nano sized particles and the band gap energy increases with increasing the cobalt (Co^{2+}) concentration in host ZnS NPs. This can be explained with the help of Burstein-Moss effect. Which says while semiconductor materials ZnS NPs are doped with transition metals with moderate concentration then the bottom of the conduction band gets populated by electrons from doped atoms for which electrons require addition energy to boost to the empty state in conduction band from valence band. As a result, band gap (E_g) gets widen [3]. In addition, the widen of band gap can also be interpreted by devolution of band bending effect.

Table2: Evaluated optical gap (E_g) of without and with Co concentrated ZnS-NPs.

Co concentration	Band gap energy (eV)
Undoped (Figure 3A)	3.57
0.5% (Figure 3B)	3.73
1.0%(Figure 3C)	4.28
1.5% (Figure 3D)	4.45

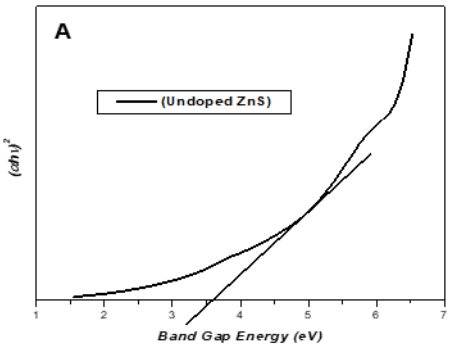

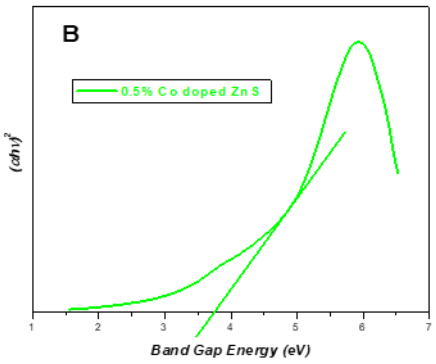

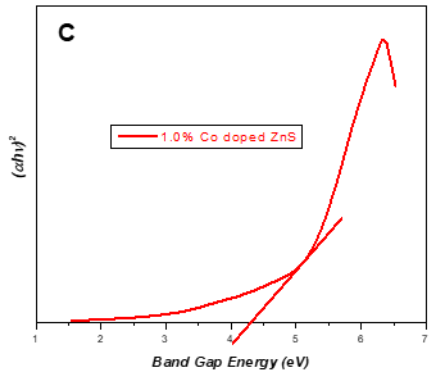

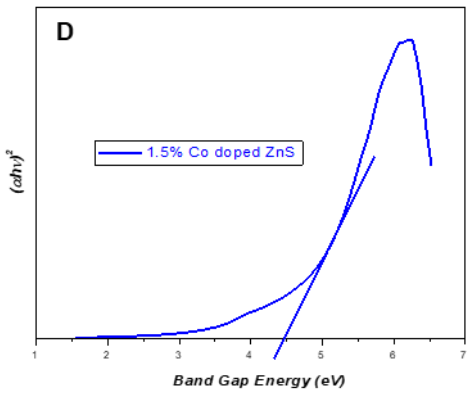

Figure 3: (a)-(d) Band gap determination from Tauc relation.

FTIR spectra analysis

To get information regarding molecular bond structure, FTIR study is very fruitful tool. In Figure 4 the qualitative analysis of FTIR spectra is shown in the range in between 4000 to 500 cm^{-1}, where we can clearly observe broad peak at 3200 to 3500 cm^{-1} owing to O-H longitudinal vibration due to stretching of absorbed excess H_2O [35]. Bands at 1628 cm^{-1} arised for Zn-S lattice [36]. Absorption bands at 1433 cm^{-1} is attributed to characteristics of hydroxyl groups of ZnS samples [37]. The highly intensed peaks at 1110 cm^{-1} indicate the Zn-S bonds for cubic structure of lattice [38]. In these FTIR spectra it has been clearly noticed with increasing cobalt amount there is no admissible change is inspected which signifies the Co^{2+}ions substituted the Zn^{2+} into host ZnS lattice without rigorous changing the crystal structure which agrees well with the XRD results.

PL study

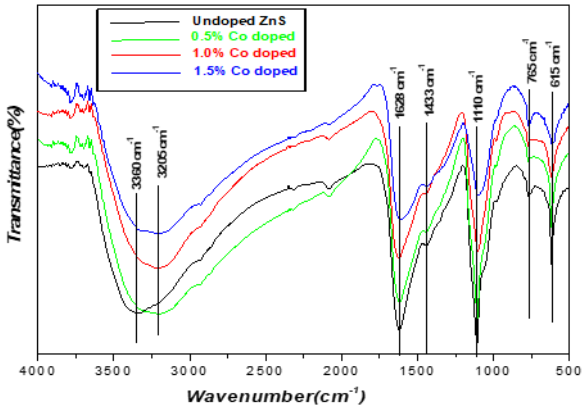

Figure 4: Spectra for FTIR of undoped and Co doped ZnS NPs.

PL studies of pure ZnS and concentrated with Co is shown in 5 no figure at room temperature where excitation wave length was 325 nm. The intense peaks appear at 388.65 nm, 386.33 nm, 384.01 nm and 380.38 nm in the violet region for pure and doping with Co (given percentage of 0.5, 1.0, 1.5) ZnS NPs respectively due to defect at lattice sites for absence of either Zn^{2+} or S^{2+}ions in host ZnS.On account of same reason, the radiative recombination process takes place in between electrons at conduction band and holes at valence band, which enables sharp intense peaks [39].

From Figure 6 at emission spectra, it can easily be noticed the blue shift occurs on increasing the cobalt concentration as compared to undoped ZnS NPs. Although, quantum confinement effect is responsible for blue shift of the emission peaks which is still not certain but it is let the blue shift could be related to narrow particle size distribution, surface defects etc. More researches are required for it [40].

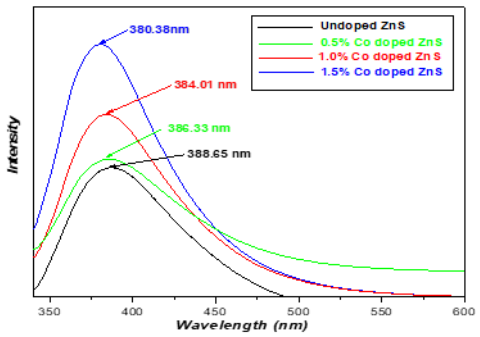

Figure 5: Photo luminance emission spectra of pure ZnS and doping with Co

SEM & EDX

Here is shown the SEM pictures of self-prepared specimens in Figure 5. We could discern a granular structure with a spherical shape from the Figures. The incorporation of Co^{2+}acquainted large assemblage in small particles. Due to acceleration towards the accumulation process the spherical shaped particle was a bit change and become overall rod like by doping Co^{2+}.Some factors are responsible for this agglomeration of nanoparticles which are doping ratio, charge distribution in the system, pH-value, chemical reactions, material solubility etc. The aggregation of two different particles generates the shrinkage of spaces between crystals. Higher Co^{2+} concentration resulted in somewhat smaller average particle sizes, indicating that colloidal nano crystal are where the growth process begins [26]. The nanoclusters grew larger spherical particles during chemical reactions, as a result further collided by secondary spherical particles and fused to produce multimeters [41]. Picture of EDX for pure and cobalt doped ZnS have been displayed in Figure no 6. Pure and contaminated with Co ZnS nanoparticles are having clearly visible peaks. The peak provided evidence that Co had been incorporated into ZnS nano particles. Stoichiometry of nanoparticles is calculated from EDX spectra using atomic and weight percentages of the

elements and this shows that the particles are almost stoichiometric.

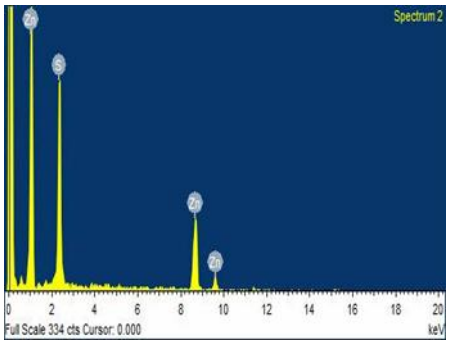

(a)

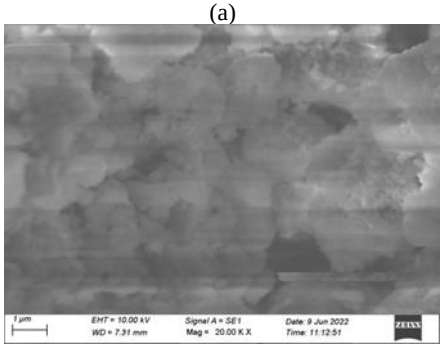

(b)

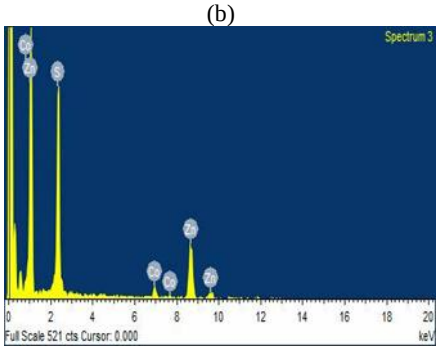

(c)

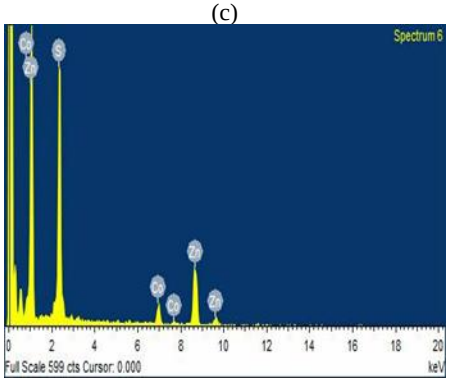

(d)

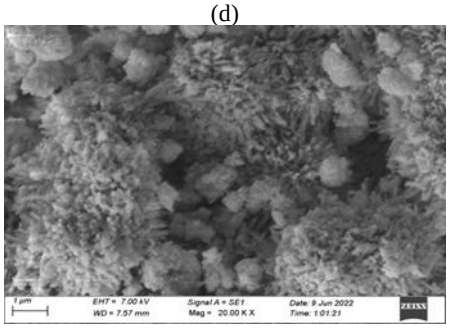

(e)

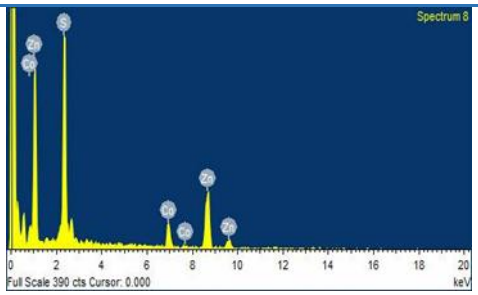

(f)

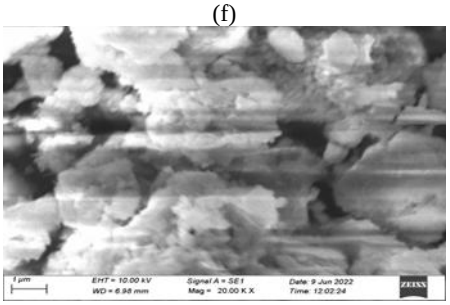

(g)

Figure 6: (a-b) SEM & EDX for pure ZnS and (c-g) doped with Co ZnS NPs

Electrical Properties

The effects of doping in ZnS NPs on the electrical parameters at room temperature were studied. The Figure 7 & 8 shows the plots of AC conductivity (σ_{AC}) and impedance (Z) the range in between frequency from 2 to 200 kHz of pure and previous mentioned percentage of doped with Co ZnS NPs. The value of σ_{AC} is measured with the help of impedance by the Equation (3)

$$\sigma_{AC} = \frac{d}{ZA} \qquad (3)$$

Where d, Z and A are representing the thickness, impedance and AC conductivity of pallet respectively. It has been noticed that for all samples,σ_{AC} shows the linear increase with the increasing frequency. Again, with rising of cobalt content in ZnS NPs, the value of σ_{AC}makes improvement with respect to undoped ZnS. This way of acting of AC conductivity of doped ZnS nanoparticles are strongly responsible for the surface defect of intermediate grain boundaries.

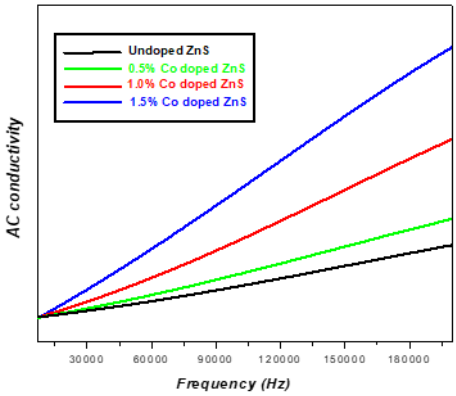

Figure 7: AC conductivity plot of ZnS and doped with Co.

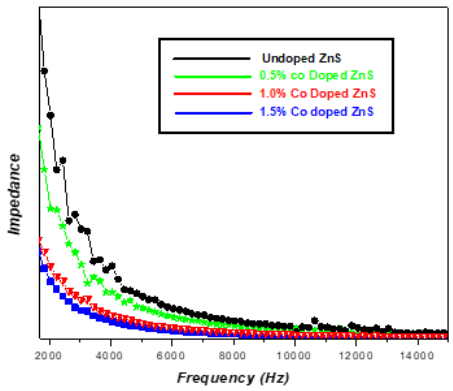

Figure 8: Impedance plot of ZnS and doped with Co doped.

In grains of conductions, the potential barriers of depletion offer interfacial resistance between the boundaries of grains which works as an insulating medium**.** At the domain of low frequency, the tunneling effect is mainly responsible for moving the carriers among the grains, in the domain of higher frequency, obtaining adequate energy containing Alternate Current electric field the carriers are able to pass through between grains of interfacial potential barriers for which their mobility becomes increased as a result the compressive improvement of σ_{AC} with enhancing the frequency [42-43].

Conclusion

In this work by hydrothermal method ZnS NPs doped with cobalt (transition metal) were successfully synthesized on a trot with changing the ratios of Co content. The structural characterization of these nanoparticles was observed the cubic structures with well-defined peaks for diffraction which are supported by standard JCPDS card. No distinguished peak has been observed for Co doping. The particle sizes of pure and ZnS doped with Co NPs had been calculated by using Debye Scherrer formula. From where it can be found on increasing the quantity of Co into ZnS, crystalline size reduces gradually. The value of optical gap evaluated from Tauc plot and it gets widen with rising the dopant contents which confirms the blue shift phenomenon. No prominent changes observed in FTIR spectra of the all samples determines the Co^{2+} ions replace Zn^{2+} ions in lattice site. In PL spectra one can see the intense peaks appear at violet region where greater is the molar concentration of cobalt lower is the wavelength and higher is the peak intensity which also supports the blue shift. In addition to study of dielectric properties of Co doped ZnS NPs degradation the depletion potential in grain boundaries as increasing Co concentration with respect to undoped ZnS which results, decreasing the dielectric constant improving AC conductivity at higher frequency region. The emitted spectra and tuning optical gap of ZnS doped with Co can be employed the materials for applying numerous applications.

References

1. B Poornaprakash, U Chalapathi, P T Poojitha, S V Prabhakar Vattikuti and S H Park, J. of Supercon. and Novel Magne. 33, 539 (2020).
2. M T Pham, N X Ca, P N Loan, N Tran, B T Huy, N T Dang et al, J. of Supercon. and Novel Magne. 32, 1761 (2019).
3. S Elsi, S Mohanapriy and K Pushpanathan, J. of Supercon. and Novel Magne. 33, 3223 (2020).
4. R Abolghasemi, R Rasuli and M Alizadeh, Mater. Today Commun. 22, 100827 (2020).
5. H Zhao and F Rosei, Chemistry 3, 229 (2017).
6. P Bhattacharya, K K Kamath, J Singh, D Klotzkin, J Phillips, H-T Jiang et al, IEEE Transac. On Electron Device 46, 871 (1999).
7. I C Sandall, C L Walker, P M Smowton, T Badcock, D J Mowbray, H Y Liu et al, Conf. Lasers Electro-Optics 2006 Quantum Electron 2006 Laser Sci. Conf. CLEO/QELS 45, 1 (2006).
8. H Shoji, Y Nakata, K Mukai, Y Sugiyama, M Sugawara, N Yokoyama et al, Appld. Phys. Lett. 71, 193 (1997).
9. M Grundmann, N N Ledentsov, N Kirstaedter, F Heinrichsdorff, A Krost, D Bimberg et al, Thin Solid Films 318, 83 (1998).
10. S K Das, S Parvin, U Honey, Md S Rana, N Jewena, J I Khandaker et al, J. of Mate. Sci. and Eng. A 10 (5-6), 103 (2020).
11. N Eryong, L Donglai, Z Yunsen, B Xue, Y Liang, J Yong et al, Appl. Surface Sci. 257, 8762 (2011).
12. F A La Porta, J Andre, M S Li, J R Sambrano, J A Varela and E Longo, Physi. Chem. Chemical Phys.16, 20127 (2014).
13. V Ramasamy, K Praba and G Murugadoss, Spectrochimica Acta Part A Molecu. Biomol. Spectro. 96, 963 (2012).
14. P Chandra and P P C Srivastava, J. of Mate. Sci. 49, 6012 (2014).
15. S Kumar, P Mandal, A Singh, S Husain, D Kumar, V K Malik et al, J. of Alloys and Comp. 830, 154640 (2020).
16. B Poornaprakash, U Chalapathi and S Park, J. of Mater. Sci.: Mater. In Electronics 28, 3672 (2017).
17. I Lopez Quintas, E Rebollar, D Ávila-Brande, J G Izquierdo, L Bañares, C Díaz Guerra et al, Nanomaterials 10, 1 (2020).
18. F J Rodriguez, J Reyes, D Y Medina, M A Barron and C Haro-Perez, Open J. of Appl. Science 09, 613 (2019).
19. S Sambasivam, B K Reddy, A Divya, N Madhusudhana Rao, C K Jayasankar and B Sreedhar, Phys. Letter A 373, 1465 (2019).
20. X Zeng, J Zhang, F Huang, X Zeng, J Zhang and F Huang, J. of Appl. Phys. 111, 123525 (2012).

21. K Sharma, P Kumar, G Verma and A Kumar, Optik (Stuttg) 206, 164357 (2020).
22. D Sridevi and K V Rajendran, Chalcogenide Letters 7, 397 (2010).
23. G Gurung, T K Ekanayaka, A J Yost and T R Paudel, Material Research Express 6, 126550 (2019).
24. B Poornaprakash, P T Poojitha, U Chalapathi, K Subramanyam and S Park, Physica E 83, 18 (2016).
25. P Mukherjee, C M Shade, A M Yingling, D N Lamont and D H Waldeck, The J. of Physical Chem. A 115, 4031 (2011).
26. I Devadoss and S Muthukumaran, J. of Mater. Sci.: Mater. In Electronics 27, 7389 (2016).
27. A Goktas and I H Mutlu, J. of Electronic Mater. 45, 11 (2016).
28. Z K Heiba, M B Mohamed and A Badawi, Chemical Phys. Letters 775, 138653 (2021).
29. K Byrappa and T Adschiri, Progr. in Crystal Growth and Charac. Of Mater. 53 2, 117 (2007).
30. L Wang, J Dai, X Liu, Z Zhu, X Huang and P Wu, Ceramics International 38 3, 1873 (2012).
31. A Goktas and I H Mutlu, J. of Sol Gel Scien. and Tech. 69, 120 (2014).
32. A L Patterson, Physical Review 56, 978 (1939).
33. J Tauc, Optical properties of Solids Abeles North Holland Amsterdam (1972).
34. J Kaur, M Sharma and O P Pandey, Optical Materials 47, 7 (2015).
35. U D Godavarti, P Nagaraju, V Yelsani, Y Pushukuri, P S Reddy amd M Dasari, J. of Semicond. 42, 122901 (2021).
36. P Sakthivel and S Muthukumaran, Optics and Laser Techn. 103, 109 (2018).
37. B Poornaprakash, D A Reddy, G Murali, N M Rao, R P Vijayalakshmi and B K Reddy, J. of Alloys & Comp. 577, 79 (2013).
38. R O Kagel and R A Nyquist, Infrared spectra of inorganic compounds (3800–45 cm−1) (1971).
39. Y C Corrado, F O Jiang, M Kozina, F Bridges and J Z Zhang, J. of Physical Chem. A 113, 3830 (2009).
40. R Zamiri, B Singh, M S Belsley and J M F Ferreira, Ceramics Internat. 4, 6031 (2014).
41. M S Samuel, J Koshy, A Chandran and K C George, Physica B: Conden. Mat. 406 (15–16), 3023 (2011).
42. N Karar, F Singh and B R Mehta, J.of Appl. Phys. 95, 656 (2004).
43. P K Ghosh, Sk F Ahmed, S Jana and K K Chattopadhyay, Optical Materials 29, 1584 (2007).